

Cobalt-bearing sulfide assemblages from the Shinkolobwe deposit, Katanga, Zaire

JAMES R. CRAIG

*Virginia Polytechnic Institute and State University
Blacksburg, Virginia 24061*

AND DAVID J. VAUGHAN

*University of Aston in Birmingham
Birmingham B47ET, England*

Abstract

Cattierite (CoS_2) specimens from the type locality contain disulfides deposited in the sequence pyrite (<0.9 percent Co) \rightarrow cobaltiferous pyrite (15–20 percent Co) \rightarrow cattierite (3.5–6 percent Fe and 2–8 percent Ni). Cattierite formation was accompanied by deposition of a Ni-rich carrollite ($\text{Co}_{1.78}\text{Fe}_{0.02}\text{Ni}_{0.62}\text{Cu}_{0.59}\text{S}_4$) which extends the range of known thiospinel compositions.

The Copperbelt of Zaire and Zambia represents the greatest known concentration of cobalt-bearing sulfides in the world. Carrollite, CuCo_2S_4 , is one of the principal cobalt ore minerals of the area, but cobalt is also known to occur in the form of cattierite (CoS_2) and cobaltian pyrite [$(\text{Fe},\text{Co})\text{S}_2$]. Cattierite was first described as a mineral species in the ores of the Shinkolobwe deposit, Zaire (formerly the Belgian Congo) by Kerr (1945). Cattierite has also been noted in the Rokana South orebody (Notebaart and Vink, 1972). Homogeneous cobalt-iron disulfides covering the complete compositional range CoS_2 to FeS_2 have been reported from Chibuluma by Riley (1965, 1968); in a few of these samples, kindly loaned by Mr. Riley, chalcopyrite is the only phase coexisting with the disulfide. Cobalt zoning in pyrite has been described from the Chibuluma deposit of the Copperbelt by Brown and Bartholomé (1972) and others. Petruk *et al.* (1969) have described some zoned bravoites in which the most cobalt-rich portion has a composition of $\text{Co}_{0.8}\text{Ni}_{0.1}\text{Fe}_{0.1}\text{S}_{1.8}$.

As part of a study of the phase relations and mineral associations of copper-cobalt sulfides (Craig *et al.*, 1978), we have had the opportunity of examining two cattierite-bearing specimens (Smithsonian Institution NMNH #107460 and #106811) from the Shinkolobwe deposit. These specimens, portions of which are shown in Figures 1 and 2, are very similar in terms of grain size, partings, and mineral content

to those described by Kerr (1945). In addition to the cattierite, both samples contain cobaltian pyrite, and one sample (#107460) contains a coexisting thiospinel which is no doubt the same as that noted by Kerr (1945) as "pale corinthian pink" and identified by him as a Co,Ni,Fe member of the linnaeite-polydymite series.

We have reexamined these phases and determined their compositions by means of the electron microprobe, a tool not available to Kerr (1945). The analysis was performed with an automated ARL-SEM-Q microprobe operated at 15 kV accelerating voltage and 0.15 microamp sample current, and using synthetic Co_3S_4 , NiS, FeS, and Cu_5FeS_4 as standards. On freshly-polished samples, the color differences between the cattierite, the cobaltian pyrite, and the thiospinel are distinct yet slight, and correspond in the disulfides to the sequence noted by Richards (1965) and Brown and Bartholomé (1972); that is, darker tints indicate increasing cobalt content. We found, however, that deposition of a carbon film approximately 250Å thick prior to microprobe analysis greatly enhanced color differences by changing the cattierite to dove gray, the thiospinel to pale tan-brown, cobaltian pyrite to pink, and pyrite to orange.

In NMNH #107460 the textural relationships between the phases—cattierite, cobaltiferous-pyrite, pyrite, and thiospinel—are illustrated in Figure 1, and their respective compositions are given in Table 1.

Table 1. Electron microprobe analyses of disulfide and thiospinel from Shinkolobwe, Zaire

(a) NMNH #107460							(b) NMNH #106811																									
wt. percent							mole percent				wt. percent							mole percent														
Co	Fe	Ni	Cu	S	Total		CoS ₂	FeS ₂	NiS ₂	CuS ₂	Co	Fe	Ni	Cu	S	Total	CoS ₂	FeS ₂	NiS ₂	CuS ₂												
Pyrite																																
0.14	46.7	0.0	0.06	53.4	100.3		0.3	99.6	0.0	0.1	0.26	44.9	0.0	1.97	53.2	100.5	0.5	95.8	0.0	3.7												
0.03	46.5	0.0	0.71	54.0	101.2		0.1	98.6	0.0	1.3	0.91	44.2	0.0	2.12	53.6	100.8	1.8	94.2	0.0	4.0												
0.14	47.0	0.0	0.03	54.0	101.2		0.3	99.7	0.0	0.1	0.14	45.3	0.0	1.52	53.8	100.7	0.3	96.9	0.0	2.9												
0.36	46.9	0.0	0.0	53.9	101.2		0.7	99.3	0.0	0.0	0.27	45.2	0.0	1.27	52.6	99.3	0.6	97.1	0.0	2.4												
0.29	46.5	0.0	0.31	53.6	100.7		0.6	98.9	0.0	0.6	0.16	45.9	0.0	0.54	52.9	99.5	0.3	98.7	0.0	1.0												
0.05	46.7	0.0	0.0	52.8	99.5		0.1	99.9	0.0	0.0	0.39	45.1	0.0	1.51	52.5	99.5	0.8	96.4	0.0	2.8												
0.05	46.9	0.0	0.0	52.9	99.8		0.1	99.9	0.0	0.0	Cattierite																					
0.11	47.0	0.0	0.0	53.0	100.2		0.2	99.8	0.0	0.0	41.7	4.53	1.17	0.23	52.6	100.2	87.1	10.0	2.5	0.4												
Cobaltiferous Pyrite																																
17.9	28.7	0.64	0.0	53.3	100.6		36.7	62.0	1.3	0.0	42.3	4.13	1.22	0.22	52.5	100.4	88.0	9.1	2.5	0.4												
16.1	30.1	0.95	0.0	53.4	100.6		33.0	65.0	2.0	0.0	41.2	4.34	1.05	0.18	51.5	98.3	87.7	9.7	2.2	0.4												
14.8	32.1	0.35	0.0	53.0	100.2		30.2	69.1	0.7	0.0	40.6	4.78	1.08	0.22	51.3	98.0	86.5	10.7	2.3	0.4												
20.7	25.0	1.80	0.0	52.3	99.8		42.4	53.9	3.7	0.0																						
15.8	30.5	0.90	0.0	52.5	99.7		32.3	65.8	1.8	0.0																						
18.6	28.3	0.78	0.0	52.8	100.5		37.8	60.6	1.6	0.0																						
16.7	29.5	1.18	0.03	53.2	100.5		34.1	63.5	2.5	0.0																						
Cattierite																																
37.6	3.89	5.71	0.53	52.7	100.3		78.4	8.6	12.0	1.0																						
38.9	4.55	3.61	0.53	52.6	100.2		81.4	10.0	7.6	1.0																						
41.4	3.89	2.01	0.18	52.9	100.5		86.8	8.6	4.2	0.3																						
40.7	4.36	2.07	0.22	52.5	99.9		85.5	9.7	4.4	0.4																						
40.2	4.43	2.09	0.18	52.1	99.0		85.3	9.9	4.5	0.4																						
39.9	4.72	2.33	0.21	52.3	99.5		84.2	10.5	4.9	0.4																						
40.0	3.94	3.05	0.21	52.3	99.5		84.4	8.8	6.5	0.4																						
40.2	4.81	2.08	0.20	51.9	99.2		84.6	10.7	4.4	0.4																						
40.4	4.97	2.59	0.11	51.9	100.0		83.6	10.8	5.41	0.2																						
wt. percent							mole percent																									
Co	Fe	Ni	Cu	S	Total		Co ₃ S ₄	Fe ₃ S ₄	Ni ₃ S ₄	Cu ₃ S ₄																						
Thiospinel																																
34.0	0.30	11.6	12.3	41.5	99.8		59.3	0.6	20.3	19.9																						
33.7	0.35	11.4	12.1	41.1	98.7		59.4	0.7	20.3	19.8																						
34.4	0.30	11.7	10.5	41.7	98.6		61.2	0.6	20.9	17.3																						
34.1	0.40	12.2	12.1	41.7	100.5		58.8	0.6	21.1	19.4																						
34.2	0.35	11.8	12.4	41.6	100.5		59.1	0.5	20.5	19.9																						
34.2	0.30	11.8	13.0	41.8	101.1		58.4	0.7	20.3	20.6																						
34.4	0.40	11.7	13.3	42.0	101.7		58.4	0.7	19.9	20.9																						
34.1	0.36	12.0	12.2	41.9	101.4		59.0	0.7	20.8	19.6																						

The disulfide occurs as three distinct, crudely concentrically disposed phases with a Ni- and nearly Co-free pyrite surrounded by a slightly nickelian cobaltian pyrite, which is in turn surrounded by nickel-

and iron-bearing cattierite. The cattierite is characterized by a well-developed (111?) parting, which is either absent or very much less developed in the pyrite and cobaltian pyrite. The thiospinel (Co_{1.78}Fe_{0.02}Ni_{0.62}Cu_{0.59}S₄) could be described as a nickelian carrollite or a cuprian siegenite, as it lies approximately midway between the ideal compositions of these minerals (Fig. 3). The composition, with approximately 12 weight percent of both nickel and copper, does not lie along any established thiospinel solid-solution series and extends the range of known natural thiospinel compositions. Fletcherite, a recently described thiospinel, also contains major amounts of the same cations but has a dominance of copper and nickel over cobalt (Craig and Carpenter, 1977). The compositions of the thiospinels represented by the solid dots on Figure 3 are tabulated in Craig *et al.* (1978). The paragenesis in NMNH #107460 appears to be pyrite → cobaltiferous-pyrite → cattierite + thiospinel. The sharp boundaries between compositionally-distinct zones of disulfide suggest that the depositing solu-

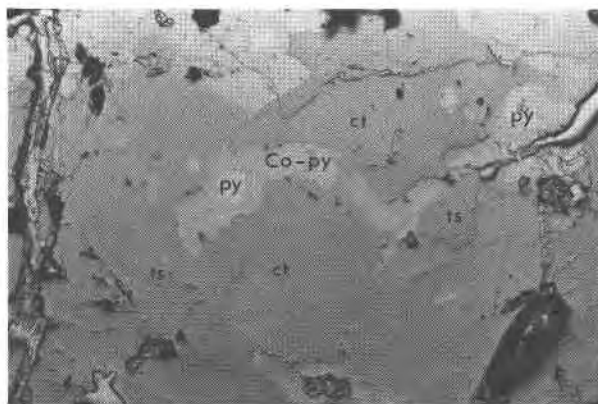


Fig. 1. NMNH #107460 from Shinkolobwe Mine. The abbreviations are: py-pyrite; Co-py-cobaltian pyrite; ct-cattierite; ts-thiospinel.

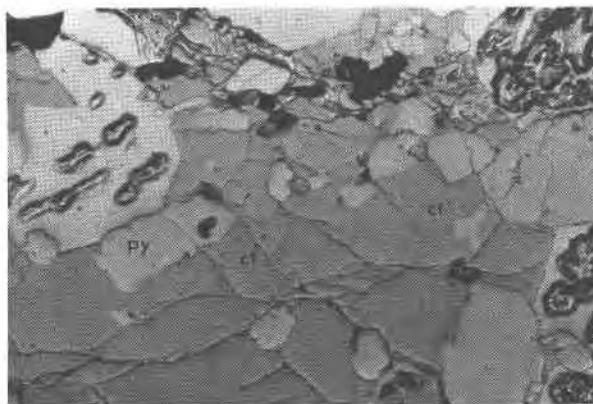


Fig. 2. NMNH #106811 from Shinkolobwe Mine. The abbreviations are: py-pyrite; ct-cattierite.

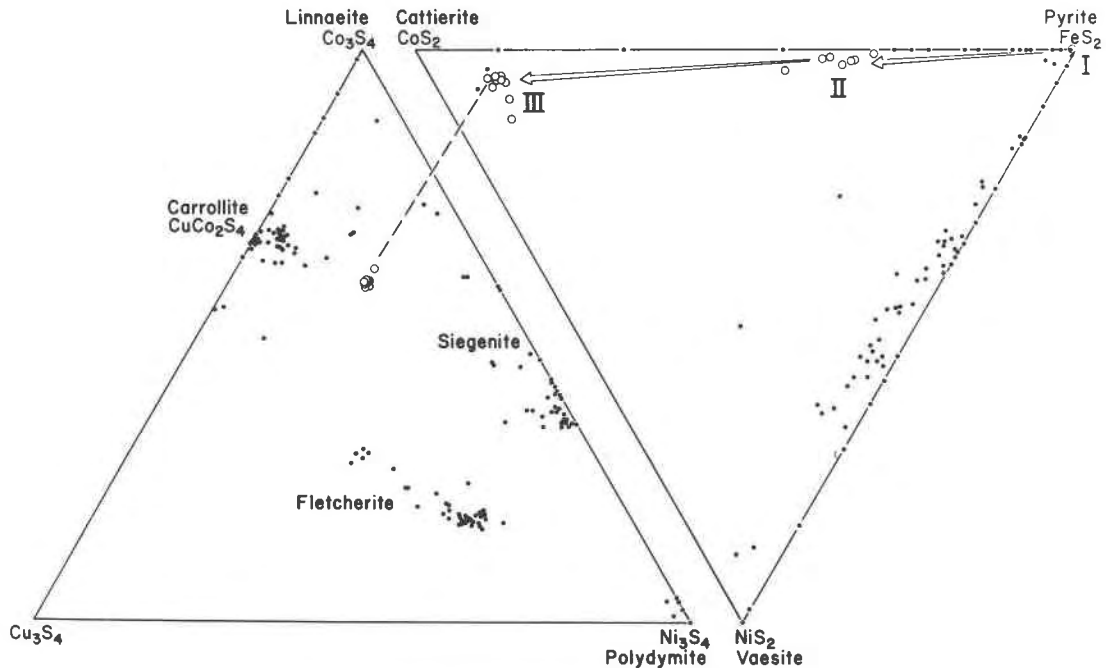


Fig. 3. The compositions of the disulfides in the three paragenetic zones in #107460 and the thiospinel coexisting with the stage III catterite are shown by the open circles. The arrows indicate the apparent paragenetic sequence from stage I (pyrite) to stage II (cobaltian pyrite) to stage III (catterite + thiospinel joined by the dashed line). The compositions of other reported disulfides and thiospinels are indicated by the dots. All compositions are in mole percent. (Figure adapted from Vaughan and Craig, 1978.)

tions changed sequentially but dramatically during sulfide formation. Grimmer (1962) has suggested that catterite and cobaltian pyrites may have formed as a result of the metamorphism of pyrite and linnaeite. However, the textures and sharp compositional boundaries of the disulfides in NMNH #107460 indicate little or no metamorphically induced changes.

In NMNH #106811 (Fig. 2, Table 1), only two phases, iron- and slightly nickel-bearing catterite and nickel- and nearly cobalt-free pyrite, are present. Both minerals occur as subhedral grains but without any clear paragenetic relationship. The absence of any concentric zoning and the interspersed nature of the pyrite and catterite suggest that both phases were simultaneously deposited from solution.

Klemm (1965) has presented phase diagrams indicating that complete solid solution exists between FeS_2 and CoS_2 only above 600°C . There is no evidence to suggest that any Copperbelt ores, including those at Shinkolobwe, were deposited at, or subsequently subjected to, temperatures even approaching 600°C . Thus if Klemm's diagrams represent equilibrium, then the naturally occurring intermediate FeS_2 - CoS_2 compositions reported by previous authors and in this work represent metastable phases. Metastability in naturally occurring disulfides has

been suggested for fukuchilite, Cu_3FeS_4 (Shimazaki and Clark, 1970), and for bravoite, $(\text{Fe},\text{Ni})\text{S}_2$ (Shimazaki, 1971; Springer *et al.*, 1964). In spite of the possible metastability of the cobaltian pyrite, it is likely that the markedly different chemical content of the paragenetic zones in NMNH #107460 indicates distinct changes in the nature of the ore-forming solutions from Fe- to (Fe + Co)- to (Co + Fe + Ni)-bearing. Only during the last stage did thiospinel precipitation accompany disulfide formation. The preferential concentration of cobalt in the disulfide rather than in the thiospinel, while the reverse is observed for the Ni^{2+} , is compatible with the stability gained by cobalt which occurs as low-spin Co^{2+} in CoS_2 (Vaughan and Craig, 1978).

The apparent depositional sequence of pyrite \rightarrow cobaltian pyrite \rightarrow catterite + thiospinel is consistent with that noted by Brown and Bartholomé (1972) and previous investigators, and thus may have been the depositional sequence throughout the Copperbelt.

Acknowledgments

We are grateful to the Smithsonian Institution for the samples on which this report is based, and acknowledge the support of NATO grant 966 and NSF grant DMR75-03879. The critical reviews by J. S. White and J. F. Riley have been most helpful.

References

- Brown, A. C. and P. Bartholomé (1972) Inhomogeneities in cobaltiferous pyrite from the Chibuluma Cu-Co deposit, Zambia. *Mineral. Deposita*, 7, 100-105.
- Craig, J. R. and A. B. Carpenter (1977) Fletcherite, $\text{Cu}(\text{Ni},\text{Co})_2\text{S}_4$, a new thiospinel from the Viburnum Trend (New Lead Belt), Missouri. *Econ. Geol.*, 72, 480-486.
- , D. J. Vaughan and J. B. Higgins (1979) The Cu-Co-S system and mineral associations of the carrollite (CuCo_2S_4)-linnaeite (Co_3S_4) series. *Econ. Geol.*, in press.
- Grimmer, A. (1962) Mineralogische und paragenetische Untersuchungen an einigen Sulfiden des Kobalts und Nickels. *Bergakademie*, 14, 296-302.
- Kerr, P. F. (1945) Catterite and vaesite: new Co-Ni minerals from the Belgian Congo. *Am. Mineral.*, 30, 483-497.
- Klemm, D. D. (1965) Synthesen und Analysen in den Driecksdiagrammen FeAsS-CoAsS-NiAsS und $\text{FeS}_2\text{-CoS}_2\text{-NiS}_2$. *Neues Jahrb. Mineral. Abh.*, 103, 205-255.
- Notebaart, C. W. and B. W. Vink (1972) Ore minerals of the Zambian Copperbelt. *Geologie en Mijnbouw*, 51, 337-345.
- Petruk, W., D. C. Harris and J. M. Stewart (1969) Langisite, a new mineral, and the rare minerals cobalt pentlandite, siegenite, parkerite and bravoite from the Langis Mine, Cobalt-Gowganda area, Ontario. *Can. Mineral.*, 9, 597-616.
- Richards, G. (1965) *Geology and Mineralization of the Copper-Cobalt Deposits of the South Orebody, Nkana, Northern Rhodesia*. Ph.D. Dissertation, Royal School of Mines, University of London.
- Riley, J. F. (1965) An intermediate member of the binary system FeS_2 (pyrite)- CoS_2 (catterite). *Am. Mineral.*, 50, 1083-1086.
- (1968) The cobaltiferous pyrite series. *Am. Mineral.*, 53, 293-295.
- Shimazaki, H. (1971) Thermochemical stability of bravoite. *Econ. Geol.*, 66, 1080-1082.
- and L. A. Clark (1970) Synthetic $\text{FeS}_2\text{-CuS}_2$ solid solution and fukuchilite-like minerals. *Can. Mineral.*, 10, 648-664.
- Springer, G., D. Schachner-Korn and J. V. P. Long (1964) Metastable solid solution relations in the system $\text{FeS}_2\text{-CoS}_2\text{-NiS}_2$. *Econ. Geol.*, 59, 475-491.
- Vaughan, D. J. and J. R. Craig (1978) *Mineral Chemistry of Metal Sulfides*. Cambridge University Press, Cambridge, England.

*Manuscript received, January 16, 1978;
accepted for publication, May 18, 1978.*